

Thermal and mechanical properties of the açai fiber/natural rubber composites

M. A. Martins · J. D. C. Pessoa · P. S. Gonçalves ·
F. I. Souza · L. H. C. Mattoso

Received: 15 December 2007 / Accepted: 26 June 2008 / Published online: 17 September 2008
© Springer Science+Business Media, LLC 2008

Abstract The açai fruit industrial processing produces a large amount of waste, mainly seeds and fibers, which is a serious environmental and public health problem. The objective of this work was to use these fibers to obtain composites with natural rubber from different clones. The effect of the addition of açai fibers and the type of clone were investigated using thermogravimetric analysis (TGA) under inert and oxidative atmospheres, differential scanning calorimetry (DSC), water sorption, and mechanical properties. The açai fibers exhibited a thermal behavior comparable to other natural fibers industrially used in polymeric composites. The addition of the fibers did not influence the thermal stability of the composites. There was no significant effect of

the type of clone and the addition of the fiber on the glass transition temperature, which was approximately -59°C for all samples. Water sorption behavior of the compounds and of the composites was similar to that of the other materials with natural rubber that are reported in the literature. The promising performance of the composites with açai fibers opens a new area of use for such fibers.

Introduction

The potential of natural fiber-based composites as reinforcement in polymers and rubber matrices has received considerable attention for their economical and ecological aspects, and their excellent specific properties [1–5]. Elastomeric composites reinforced with natural fibers are an important class of materials because of their improved physical and mechanical properties, processability, and economic advantages. These materials combine the stiffness of the fibers with the elasticity of the rubber. In developing countries, natural fiber crops are also important to generate jobs that improve social and economic conditions [6–10].

Açai (*Euterpe oleracea* Mart.) is a palm plant widely diffused and cultivated in Amazon regions especially in Pará, a state of Brazil, where the pulp of the fruit has a large consumption as beverages and in food preparations (about 180 tons/year). A wide variety of marketable products is produced from this palm, but the spherical fruits, which are mainly harvested from July to December, are its most important edible product. The juice is typically prepared by macerating the small edible pulp of the fruit, and it is used to produce energetic snack beverages, ice cream, jam, and liqueur [11–13]. Açai fruit has recently caught international interest, not only due to its novelty, taste, and exotic flavor

M. A. Martins · P. S. Gonçalves
Agronomic Institute, APTA/IAC - Av. Barão de Itapura 1481,
13020-902 Campinas, Brazil

M. A. Martins
e-mail: mariaalice@cnpdia.embrapa.br

P. S. Gonçalves
e-mail: paulog@iac.sp.gov.br

M. A. Martins · J. D. C. Pessoa
Embrapa Agricultural Instrumentation, C.P. 741, São Carlos,
SP 13560-970, Brazil

J. D. C. Pessoa
e-mail: dalton@cnpdia.embrapa.br

F. I. Souza
Embrapa Eastern Amazon, C.P. 48, 66095-100 Belém, Brazil

L. H. C. Mattoso (✉)
National Nanotechnology Laboratory for Agribusiness (LNNA),
Embrapa Agricultural Instrumentation, C.P. 741, São Carlos,
SP 13560-970, Brazil
e-mail: mattoso@cnpdia.embrapa.br

but also due to potential health benefits associated with its phytochemical composition [14–16].

The fruit is rounded, purple-black at complete maturity with a diameter of 10–20 mm. It contains one light brown seed, which is about 80% of the fruit size, and is covered with a layer of rough fibers. The açai industrial processing produces a large amount of waste, mainly seeds and fibers [11, 17]. It is estimated that only in the capital of Pará state, Belém, approximately from 100,000 to 120,000 tons of fruits are worked up commercially per year, yielding around 100,000 tons of residues [18, 19]. The growing amount of waste has resulted in a serious environmental and public health problem.

The aim of this work was to use the açai fibers, the waste of industrial process, to obtain composites with a natural rubber matrix from different clones. The effect of the addition of açai fibers and the type of clone have been investigated using thermogravimetric analysis (TGA), differential scanning calorimetry (DSC), water sorption, and mechanical properties.

Experimental

Materials

Açai fibers were supplied by Embrapa Western Amazonia National Research Center in Belém/Brazil. They were manually removed from the fruit, and manually chopped, so that 10 mm long fibers were obtained.

Natural rubber latices from *Hevea brasiliensis* (Willd. ex A. de Juss.) Muell.-Arg. of three clones: GT 1 (Gondang Tapen), IAN 873 (Instituto Agrônômico do Norte), and RRIM 600 (Rubber Research Institute of Malaysia), an old popular clone (used as a control), were obtained from Northwest Regional Pole in Votuporanga city, an experimental plantation. The natural rubber clones were grown in the plateau region of São Paulo state, Brazil, whose coordinates and ecological conditions are [20]: 20°25' S, 49°50' W, altitude 450 m; mean temperature during growing season 32 °C; mean annual rainfall 1,480 mm, with a hot wet summer and a dry winter with low temperature and rainfall; Paleudalf soil, with average nutrient status and poor physical structure.

Natural rubber latices were collected, and the stabilization of the samples in the field was done using 4.7 mL of NH₄OH for 100 mL of latex. The samples were coagulated with 3 mol·L⁻¹ acetic acid solution and dried.

Methods

Composites containing 5% and 10% of raw açai fibers were prepared in a two-roll open mixing mill according to Table 1. The mixing time and the number of passes were maintained for all mixtures. Randomly oriented composite

Table 1 Formulations of the mixes

Components	(phr)
Natural rubber	100
Stearic acid	3
Zinc oxide	5
Antioxidant ^a	1
Carbon black	10
Processing oil ^a	5
Accelerators ^a	2
Sulfur	2.5

^a Oil: Dutrex 718NC (Shell); accelerators: TMTD and MBTS; antioxidant: Vulcanox BHT (Bayer)

sheets (150 × 160 × 3 mm) were vulcanized by hot-press molding at 4 MPa, at 145 °C for 5 min.

Thermogravimetric analysis was obtained in a TA Instruments model Q500, in the temperature range from 25 °C to 800 °C, at a heating rate of 10 degree/min. in inert (nitrogen) and oxidative (synthetic air) atmospheres, with a flow rate of 60 mL·min⁻¹. Approximately 10 mg were used for each sample preparation.

The glass-transition temperature (T_g) of the samples (ca. 6 mg) was measured using a DSC from a TA Instruments model Q100 with a scan rate of 10 °C/min within the temperature range from -80 °C to 80 °C, under a nitrogen atmosphere. A second scan was used to evaluate the glass transition temperature of the samples, which was determined from the mid-point of an endothermic shift of the baseline.

Mechanical tests followed ASTM D 412-92, and they were carried out using an Instron Machine at a crosshead speed of 500 mm/min. Samples were conditioned at 20 ± 2 °C and 50 ± 5% relative humidity for at least 48 h before testing.

SEM analyses were performed with a Zeiss DSM 960 instrument, operating at 20 kV on samples containing a thin layer (ca. 15 nm) of sputter-coated gold.

Water sorption was determined according to the following procedure: samples were weighed (M_{initial}) and fully immersed in water at 25 °C for up to 7 days. They were taken out of the water at regular intervals, wiped free of surface moisture with a dry cloth, weighed immediately (M_{final}), and then repositioned in the water. Percentage increase in mass during immersion was calculated according to the equation:

$$\text{Mass \%} = [(M_{\text{final}} - M_{\text{initial}}) / M_{\text{initial}}] \times 100$$

where mass % is the total of increase in mass, M_{initial} is the initial sample mass, and M_{final} is the mass of the sample after immersion in water.

Results and discussion

Figure 1 shows typical TG and DTG curves obtained for the compounds and composites with açai fibers in inert

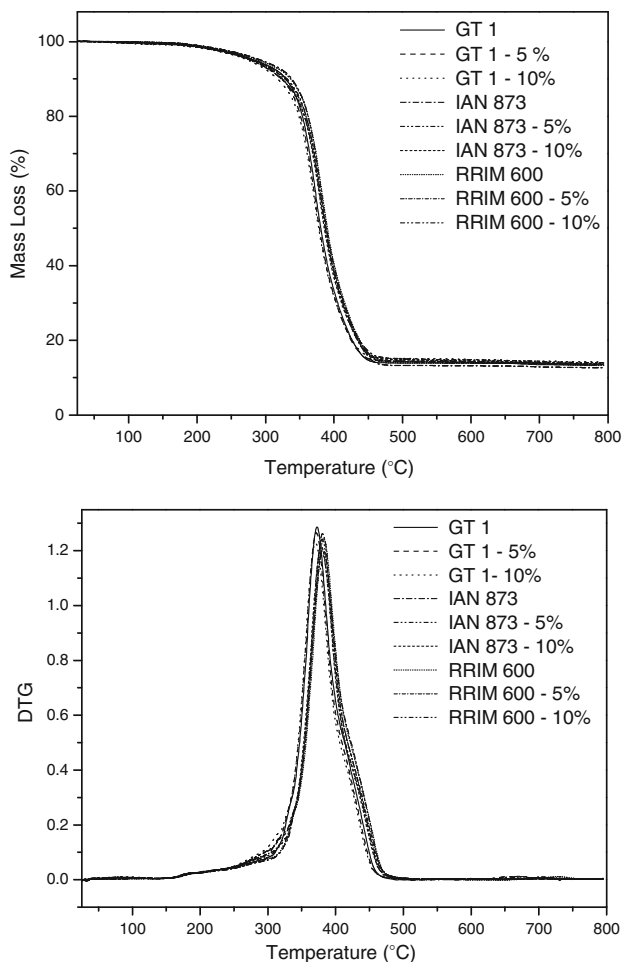


Fig. 1 TG and DTG curves of the compounds from different clones of natural rubber (GT 1, IAN 873, and RRIM 600), and the composites with 5% and 10% of açai fibers, nitrogen atmosphere

atmosphere. TG and DTG curves of all clones evaluated have shown the same general shape, suggesting that the decomposition mechanism is the same. It can be seen that the TG curves have only one large plateau and that the DTG curve has one degradation peak, indicating that thermal degradation is a one-stage reaction, ranging from approximately 300 °C to 450 °C. The mass loss is of about 85%, and it can be assigned to the thermal decomposition of the natural rubber and of the açai fibers. The temperature of the maximum mass loss rate of the samples, corresponding to the peak temperature of the DTG curves is around 375 °C for the compound and composites with GT 1 clone and approximately 385 °C for the other samples. No significant differences in the thermal stability among samples up to around 300 °C could be observed.

The temperature at which 50% decomposition occurs is generally considered as an index of thermal stability [21]. This temperature is about 375 °C for the compound and composites with GT 1 clone and approximately 390 °C for the other samples, indicating that only the natural rubber

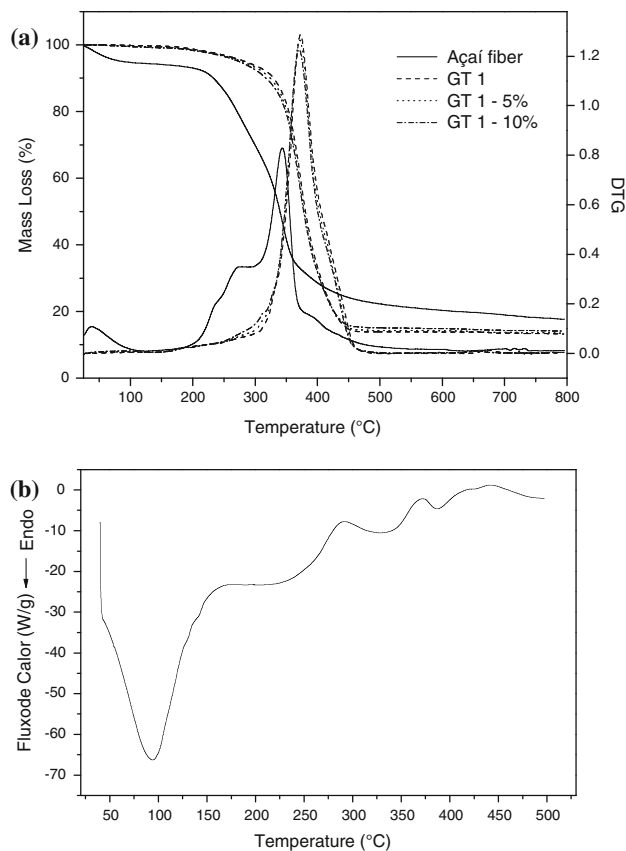


Fig. 2 TG/DTG curves of the açai fiber, the GT 1 compound, and the composites with natural rubber from GT 1 clone with 5% and 10% of açai fibers in nitrogen atmosphere (a), and DSC curve of açai fiber (b)

from IAN 873 clone has thermal stability comparable to the well-established Malaysian clone, RRIM 600. From 450 °C, the remained content of residues was about 15% for all samples.

Figure 2a shows typical TG/DTG curves for the açai fibers and the composites with GT 1 clone, for instance. The fibers have shown good stability up to around 230 °C and have a three-degradation-step process in inert atmosphere. The DTG curve shows an initial peak between 50 and 100 °C, which corresponds to water loss. After this peak, the first decomposition peak at about 270 °C is attributed to thermal depolymerization of hemicellulose and the glycosidic linkages of cellulose, and the second decomposition peak at about 340 °C is attributed to cellulose and lignin decomposition. The açai fibers exhibited a thermal behavior comparable to other natural fibers industrially utilized in polymeric composites [22–26]. Chand et al. [23] and Martins et al. [24] obtained similar results for thermal studies of the sisal fibers. It was observed that, after a small change in mass up to 100 °C attributed to the elimination of water, the main initial mass loss of sisal fibers begins at 200 °C to 310 °C [23]. Varma et al. [25] and Silva et al. [26] investigated the thermal

behavior of coir fibers. Coir fibers also exhibited an initial small mass loss as seen for the sisal, and they show a good thermal stability up to 215 °C [26]. Sisal and coir fibers showed decomposition processes and thermal stability comparable to that of the açai fibers. DSC curve of the açai fibers is shown in Fig. 2b. Açai shows an endothermic peak at around 100 °C, which is due to water loss, and exothermic peaks at higher temperatures, which are attributed to hemicellulose, cellulose, and lignin decomposition [22, 23].

The compounds and the composites show good stability up to about 300 °C, and a degradation process in one step, Fig. 2a. The temperature at which 50% decomposition occurs is the same for the compounds and the composites, about 375 °C, indicating that the addition of the fibers did not influence the thermal stability of the materials.

Figure 3a and b shows the SEM micrographs of the açai fruit and açai fibers, respectively. Açai fruits, Fig. 3a, are almost round, with diameter varying between one and two centimeters and a smooth external epidermis (peel). The round-shaped fruits appear in green clusters when immature and ripen to a dark. The seed accounts for most of the fruit size and is covered by thin fibrous fibers under which is a small edible layer (pulp). Açai beverage is typically prepared by macerating with water the edible pulp that is approximately 2.4% protein and 5.9% lipid.

Figure 3b shows the longitudinal morphology of the fibers that cover the açai seed. The morphology of the fibers is rough and parenchyma cells can be seen on the surface. Fibers in the fruits have been bound together by lignin. The chemical composition shows that açai fibers have 33% of Klason lignin, 33% of cellulose, 37% of hemicellulose, 7% of extractives in water, and 1% of organic extractives. The chemical composition of açai is comparable to the most usual values for natural fibers. Mwaikambo et al. [27] listed the chemical composition of the main natural fibers of interest such as sisal, cotton, coir, jute, flax. Among these fibers, cellulose content ranged from 13% to 92%, hemicellulose ranged from <1 to 28%, and lignin content was between 1% and 28%.

The thermal degradation of natural rubber in air is not a simple random chain scission process, but it has some side reactions that occur simultaneously [28]. During the early degradation (up to 300 °C), oxidation, crosslinking, and chain scission may occur at the same time, and the main reactions being oxidation and crosslinking. However, in this case, no significant mass loss was observed. During the late degradation (after 300 °C), the main reaction was an oxidative degradation, accompanied by the occurrence of mass loss. Oxygen generally tends to act as an oxidizing agent promoting, therefore, oxidative degradation, which is more time dependent and intense as temperature increases than that normally occurring for experiments carried out

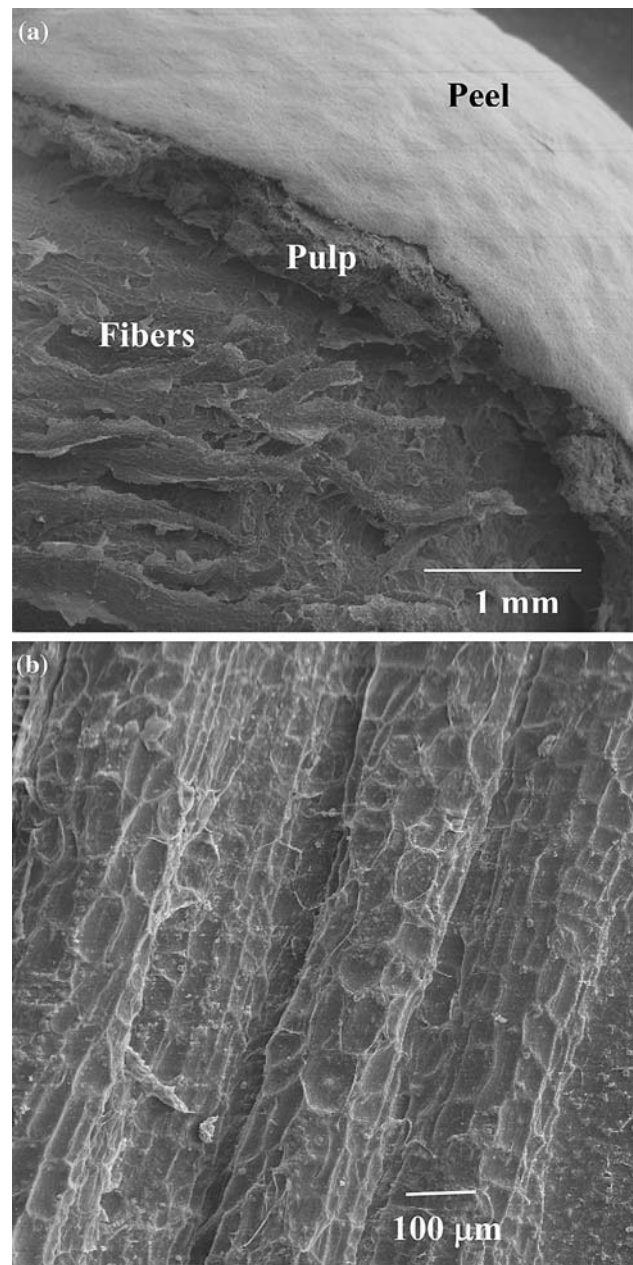


Fig. 3 Scanning electron micrographs of the açai fruit, 20× (a) and of the açai fibers, 100× (b)

under nitrogen atmosphere [28, 29]. The occurrence of two or more peaks in the DTG curves in air atmosphere indicates the formation of thermally stable intermediate products, and the absence of these peaks in nitrogen atmosphere may be due to the absence of intermediate products formed in the presence of air [21, 30, 31].

For the oxidative atmosphere, TG and DTG curves for the compounds and composites with GT 1 and RRIM 600 clones are shown in Fig. 4. Thermal degradation of the samples in synthetic air occurs in three consecutive mass losses. The first step of degradation starts at around 300 °C

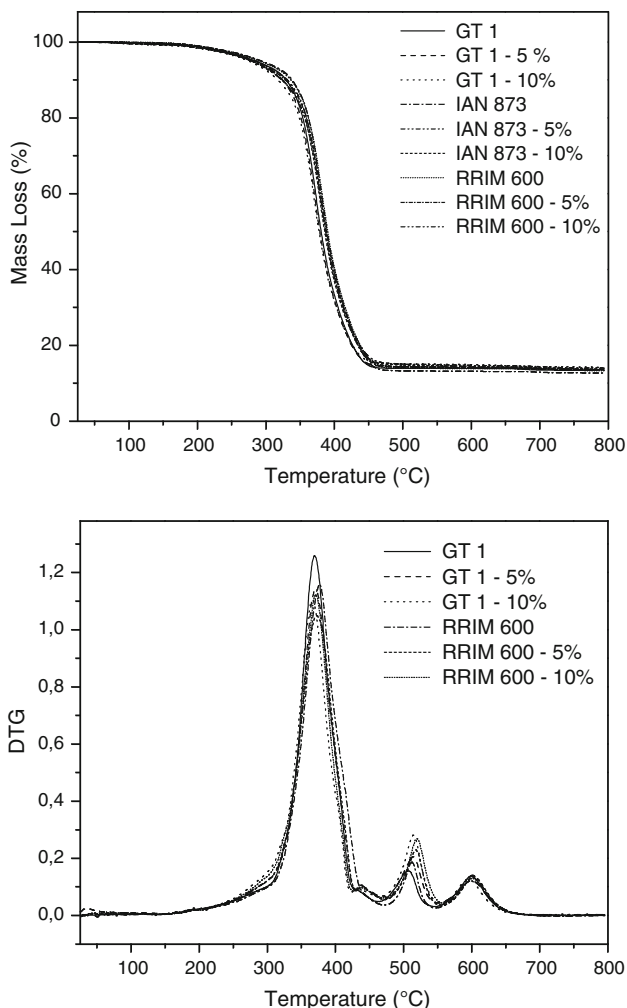


Fig. 4 TG/DTG curves of GT 1 and RRIM 600 compounds, and their composites with 5% and 10% of açai fibers in air atmosphere

and is completed at 400 °C, and the mass loss is about 73%, which can be attributed to the thermal decomposition of the natural rubber and the açai fibers. The first mass loss peak is dominating. The second mass loss peak ranges from approximately 400 °C to 535 °C; the mass loss is about 12%. For the third mass loss peak, the mass loss is around 8%, and it ranges from approximately 535 °C to 635 °C. The residue remaining after the thermooxidative degradation is about 4%. Temperature at which 50% decomposition occurs is about 380 °C for the samples with GT 1 clones and for those with the control, RRIM 600 clone, indicating that, in oxidative atmosphere, the thermal stability of natural rubber from GT 1 clones is comparable to that of the RRIM 600 clone. The decomposition process changes from one step to three steps depending on the atmosphere used.

DSC provides information concerning the enthalpy change accompanying a physical or chemical event within a material. The glass transition is a second order event, which manifests itself in a DSC curve as a step change

corresponding to the change in the heat capacity of the system [31]. The glass transition temperature (T_g) is an important parameter in polymeric applications, because it elucidates how the polymer behaves under ambient conditions. Many of the important technical properties of elastomers such as resilience and abrasion resilience can be correlated to T_g . This phenomenon is characterized by a temperature in which the material changes from the glassy to the rubbery state. Elastomers have glass transition temperatures below room temperature. Thus, elastomeric materials are rubber-like polymers at room temperatures, but below their glass transition temperature they become rigid and lose their rubbery characteristics [31, 32].

DSC curves and glass transition temperature for the samples are shown in Fig. 5 and Table 2, respectively. It can be observed that there is no significant effect of the type of clone and the addition of fiber on the results. The DSC curves show the same behavior, and the curves exhibited changes in baseline in the temperature of

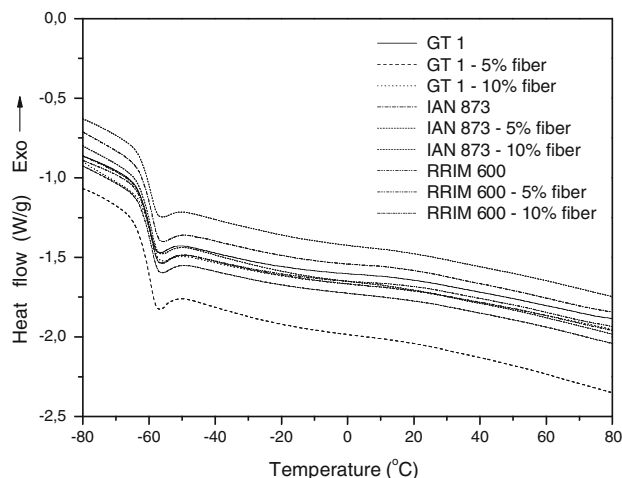


Fig. 5 DSC curves of the compounds from different clones of natural rubber (GT 1, IAN 873, and RRIM 600), and the composites with 5% and 10% of açai fibers

Table 2 Effect of the natural rubber clone on the glass transition temperature (T_g) of the composites with açai fibers

Samples	T_g (°C)
GT 1	-59.5
GT 1—5% fiber	-59.3
GT 1—10% fiber	-59.2
IAN 873	-59.2
IAN 873—5% fiber	-59.4
IAN 873—10% fiber	-59.3
RRIM 600	-58.8
RRIM 600—5% fiber	-58.9
RRIM 600—10% fiber	-59.0

approximately $-59\text{ }^{\circ}\text{C}$ for all samples, which is attributed to the glass transition temperature. These results indicate that there is no significant difference in the flexibility chain among compounds and composites, even after the addition of açai fibers. The results of the T_g values are summarized in Table 2. There are no significant differences among the T_g values of the different GT 1 and IAN 873 clones in relation to the Malaysian clone RRIM 600. The T_g values are way below the room temperature, and that is important for several technological applications.

Table 3 shows the results of mechanical properties of the natural rubber compounds and the composites with 5% and 10% of açai fibers. It can be observed that the compounds show lower modulus and higher tensile strength than the composites. It is also observed that the composites with 5% of fibers show the best balance values for mechanical properties indicating that is the best fiber load. Composites with 5% of açai fiber in RRIM 600 natural rubber matrix have shown the highest modulus results. The decrease in tensile strength at high fiber loading could be a reflection of poor adhesion between the fiber and the matrix, which promoted micro crack formation at the interface as well as non-uniform stress transfer due to the fiber agglomeration in the matrix [3].

It can also be observed that, for the tensile strength, there is no significant variation among the samples for the GT 1 and IAN 873 clones. On the other hand, for the RRIM 600, the compounds showed about 20% higher tensile strength than the composites with 5% of fibers. For the elongation, no important effects of the type of clone and the addition of the fibers could be noted, indicating that the increase in fiber loading did not lead to a stiffness and brittleness of the composites, which is in agreement with the T_g results. Addition of 5% of fibers leads to an increase of about 100% in modulus in all cases. Açai fiber/NR composites show mechanical properties comparable to the composites with other natural fibers [7, 8]. Varghese et al. [7] investigated the

effect of a two-component dry bonding system and the fiber treatment on the mechanical and viscoelastic properties of short sisal fiber reinforced natural rubber composites. It was observed that the addition of 10% of sisal fibers decreased both elongation and tensile strength, independent of the fiber treatment, fiber orientation, and the bonding system used. Tensile strength ranged from 17.3 MPa for the compound to 12.2 MPa for the composite with 10% of untreated fibers, and elongation changed from 1072% to 792%. It was also observed that composites with 35% of fiber load showed higher modulus and tensile strength than the compound. Composites of natural rubber and short jute fibers were studied by Murty et al. [8]. As observed for sisal fibers, the addition of 5% and 10% of jute reduced the elongation and tensile strength of the materials. In this study, for instance, tensile strength changed from 12.8 MPa to 7.7 MPa for the composites with longitudinally oriented fibers. It was also noted that processing properties like green strength and mill shrinkage are improved by the addition of fiber.

Stress–strain curves for the compound and the composites of the RRIM 600 clone are shown in Fig. 6. It can be seen that the compound has higher elongation and tensile strength than the composites. All curves have similar shape and show a brittle-type failure for both unfilled and reinforced specimens. The addition of the fibers decreases not only tensile strength but also elongation of the materials. In all cases, a similar behavior was observed.

The water penetration and diffusion in composites occur mainly through two possible mechanisms: water molecules either diffuse directly into the matrix and reach the fibers or enter the composites through capillary mechanism along the fiber-matrix interface, followed by diffusion from the interface into the matrix and fibers. The rate of water diffusion depends on external environments such as temperature and applied stress, as well as internal material

Table 3 Effect of the addition of açai fibers and the type of natural rubber clone on the mechanical properties

Samples	Modulus (MPa)	Tensile strength (MPa)	Elongation (%)
GT 1	2.2 ± 0.4	14 ± 6	389 ± 15
GT 1/5% fibers	4.5 ± 0.7	13 ± 3	307 ± 32
GT 1/10% fibers	3.4 ± 0.4	10 ± 2	295 ± 7
IAN 873	2.4 ± 0.1	16 ± 2	347 ± 15
IAN 873/5% fibers	5.2 ± 0.1	15 ± 1	332 ± 4
IAN 873/10% fibers	4.3 ± 0.1	13 ± 1	329 ± 10
RRIM 600	2.6 ± 0.4	19 ± 1	378 ± 21
RRIM 600/5% fibers	5.7 ± 0.4	16 ± 2	345 ± 13
RRIM 600/10% fibers	3.9 ± 0.6	12 ± 2	313 ± 20

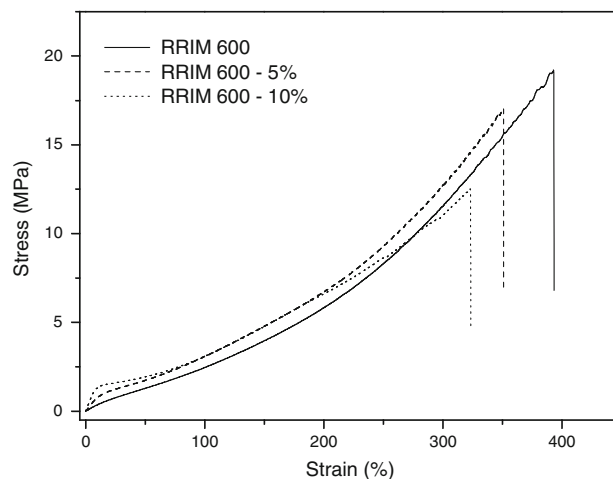


Fig. 6 Stress–strain curves of the compounds and composites with 5% and 10% of açai fibers with natural rubber from RRIM 600 clone

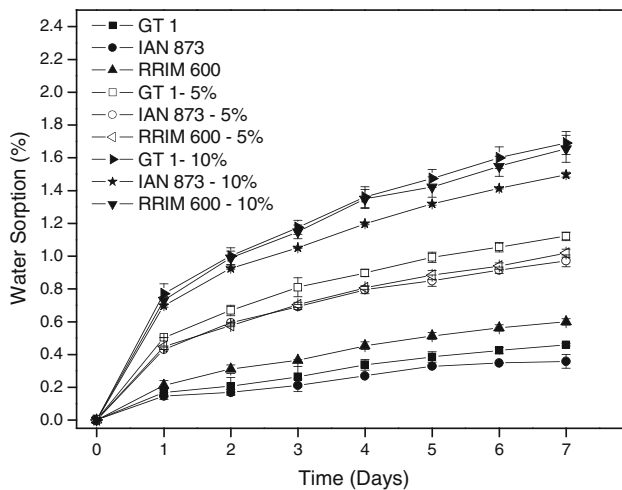


Fig. 7 Percent increase in mass as a function of the time of immersion of the compounds from different clones of natural rubber (GT 1, IAN 873, and RRIM 600), and the composites with 5% and 10% of açai fibers, room-temperature

states such as debonding at the fiber-matrix interface, matrix crack, and inherent sorption properties of the constituent materials. The extent of fiber-matrix adhesion is also an important factor in determining the sorption behavior of the composite [3, 33].

Figure 7 shows the water sorption data for the compounds and the composites with 5% and 10% of açai fiber load. As expected, the addition of açai fibers to the natural rubber increases the water sorption since the fibers are hydrophilic and porous. It can be observed that the value of the water sorption is lower for the compound than those of the composites. Also, the amount of water sorbed increases with the fiber load. Comparing the sorption of water in the compound and the composites, it is observed that on the seventh day the percentage of sorption is about three times as much as that of the first day for all samples.

The samples did not attain equilibrium water content even after seven days of water immersion. This may be due to the slow relaxation processes that occur after the initial fast diffusion process whose rates are lower than that of the diffusion [34]. For the same fiber content, there is no significant difference in the microstructure among the clones studied and the effect of addition of the fibers on the water sorption is the same for the different clones. Similar results have been obtained by Geethamma et al. [34] for the composites with coir fiber reinforced natural rubber, indicating that the açai fiber performance is comparable with the commercial natural fibers utilized, and it can be used to develop new composites materials. As it was observed to composites with açai, the composites with untreated coir fiber did not attain equilibrium water content after 200 hr of water immersion either, and the increase in fiber load led to an increase in water sorption.

Conclusions

The composites with açai fibers exhibited thermal behavior and mechanical properties comparable to those with other natural fibers industrially used in polymeric composites. The addition of the fibers did not influence the thermal stability of the composites. The decomposition process changes from one to three steps according to the atmosphere used. In inert atmosphere, only the natural rubber from IAN 873 clone has thermal stability comparable to the Malaysian clone, RRIM 600. However, in oxidative atmosphere, no significant difference was observed among the clones studied. There is no significant effect of the type of clone and the addition of fiber on the results of glass transition temperature, which is approximately -59°C for all samples. Water sorption behavior of the compounds and of the composites is similar to that of the other materials reported in the literature.

Acknowledgement The authors thank FAPESP and CNPq for their financial support.

References

- Mokoena MA, Djokovic V, Luyt AS (2004) *J Mater Sci* 39(10):3403. doi:10.1023/B:JMSSC.0000026943.47803.0b
- Mishra S, Mohanty AK, Drzal LT, Misra M, Hinrichsen G (2004) *Macromol Mater Eng* 289(11):955. doi:10.1002/mame.200400132
- Thwe MM, Liao K (2003) *J Mater Sci* 38(2):363. doi:10.1023/A:1021130019435
- Bledzki AK, Gassan J (1999) *Prog Polym Sci* 24(2):221. doi:10.1016/S0079-6700(98)00018-5
- Bisanda ETN, Ansell MP (1992) *J Mater Sci* 27(6):1690. doi:10.1007/BF00542934
- da Costa HM, Visconde LLY, Nunes RCR, Furtado CRG (2002) *J Appl Polym Sci* 83(11):2331. doi:10.1002/app.10125
- Varghese S, Kuriakose B, Thomas S, Kosh AT (1994) *J Adhes Sci Technol* 8(3):235. doi:10.1163/156856194X01086
- Murty VM, De SK (1982) *J Appl Polym Sci* 27(12):4611. doi:10.1002/app.1982.070271208
- Geethamma VG, Mathew KT, Lakshminarayanan R, Thomas S (1998) *Polymer (Guildf)* 39(6–7):1483. doi:10.1016/S0032-3861(97)00422-9
- Kumar RP, Geethakumari Amma ML, Thomas S (1995) *J Appl Polym Sci* 58(3):597. doi:10.1002/app.1995.070580315
- Gallori S, Bilia AR, Bergonzi MC, Barbosa WLR, Vincieri FF (2004) *Chromatographia* 59(11–12):739. doi:10.1365/s10337-004-0305-x
- Del Pozo-Insfran D, Brenes CH, Talcott ST (2004) *J Agric Food Chem* 52(6):1539. doi:10.1021/jf035189n
- Muñiz-Miret N, Vamos R, Hiraoka M, Montagnini F, Mendelsohn RO (1996) *For Ecol Manage* 87(1–3):163. doi:10.1016/S0378-1127(96)03825-X
- Pacheco-Palencia LA, Hawken P, Talcott ST (2007) *Food Res Int* 40(5):620. doi:10.1016/j.foodres.2006.11.006
- Pacheco-Palencia LA, Hawken P, Talcott ST (2007) *Food Chem* 105(1):28. doi:10.1016/j.foodchem.2007.03.027
- Schauss AG, Wu X, Prior RL, Ou B, Patel D, Huang D et al (2006) *J Agric Food Chem* 54(22):8598. doi:10.1021/jf060976g

17. Coisson JD, Travaglia F, Piana G, Capasso M, Arlorio M (2005) *Food Res Int* 38(8–9):893. doi:[10.1016/j.foodres.2005.03.009](https://doi.org/10.1016/j.foodres.2005.03.009)
18. Rodrigues RB, Lichtenthäler R, Zimmermann BF, Papagianopoulos M, Fabricius H, Marx F (2006) *J Agric Food Chem* 54(12):4162. doi:[10.1021/jf058169p](https://doi.org/10.1021/jf058169p)
19. Rogez H (2000) *Açaí: Preparação, composição e melhoramento da conservação*, 1st edn. EDUFPA, Brazil
20. Gonçalves PS, Silva MA, Gouvêa LRL, Scaloppi EJ, Scaloppi EJ Jr (2006) *Sci Agric* 63(3):246. doi:[10.1590/S0103-90162006000300006](https://doi.org/10.1590/S0103-90162006000300006)
21. Menon ARR, Pillai CKS, Nando GB (1996) *Polym Degrad Stabil* 52(3):265. doi:[10.1016/0141-3910\(96\)00007-9](https://doi.org/10.1016/0141-3910(96)00007-9)
22. Mwaikambo LY, Ansell MP (1999) *Angew Makromolekulare Chem* 272(1):108. doi:[10.1002/\(SICI\)1522-9505\(19991201\)272:1<108::AID-APMC108>3.0.CO;2-9](https://doi.org/10.1002/(SICI)1522-9505(19991201)272:1<108::AID-APMC108>3.0.CO;2-9)
23. Chand N, Sood S, Singh DK, Rohatgi PK (1987) *J Therm Anal* 32(2):595. doi:[10.1007/BF01912712](https://doi.org/10.1007/BF01912712)
24. Martins MA, Joekes I (2003) *J Appl Polym Sci* 89(9):2507. doi:[10.1002/app.12285](https://doi.org/10.1002/app.12285)
25. Varma DS, Varma IK (1986) *Thermochim Acta* 108:199. doi:[10.1016/0040-6031\(86\)85092-4](https://doi.org/10.1016/0040-6031(86)85092-4)
26. Silva GG, de Souza DA, Machado JC, Hourston DJ (2000) *J Appl Polym Sci* 76(7):1197. doi:[10.1002/\(SICI\)1097-4628\(20000516\)76:7<1197::AID-APP23>3.0.CO;2-G](https://doi.org/10.1002/(SICI)1097-4628(20000516)76:7<1197::AID-APP23>3.0.CO;2-G)
27. Mwaikambo LY, Ansell MP (2002) *J Appl Polym Sci* 84(12):2222. doi:[10.1002/app.10460](https://doi.org/10.1002/app.10460)
28. Li SD, Yu HP, Peng Z, Zhu CS, Li PS (2000) *J Appl Polym Sci* 75(11):1339. doi:[10.1002/\(SICI\)1097-4628\(20000314\)75:11<1339::AID-APP3>3.0.CO;2-0](https://doi.org/10.1002/(SICI)1097-4628(20000314)75:11<1339::AID-APP3>3.0.CO;2-0)
29. de Medeiros ES, Moreno RMB, Ferreira FC, Alves N, Job AE, Gonçalves PS et al (2003) *Prog Rubber Plast Recycl Technol* 19(4):189
30. Sircar AK (1997) *J Therm Anal* 49(1):293. doi:[10.1007/BF01987450](https://doi.org/10.1007/BF01987450)
31. Brazier DW (1980) *Rubber Chem Technol* 53(3):437
32. Sircar AK, Galaska ML, Rodrigues S, Chartoff RP (1999) *Rubber Chem Technol* 72(3):513
33. Sreekala MS, Kumaran MG, Thomas S (2002) *Comp Part A Appl Sci Manuf* 33(6):763. doi:[10.1016/S1359-835X\(02\)00032-5](https://doi.org/10.1016/S1359-835X(02)00032-5)
34. Geethamma VG, Thomas S (2005) *Polym Comp* 26(2):136. doi:[10.1002/pc.20086](https://doi.org/10.1002/pc.20086)